Supporting information - Open-circuit dissolution of platinum from the cathode in polymer electrolyte membrane water electrolysers

S.I.1 PEMWE cell construction

a)

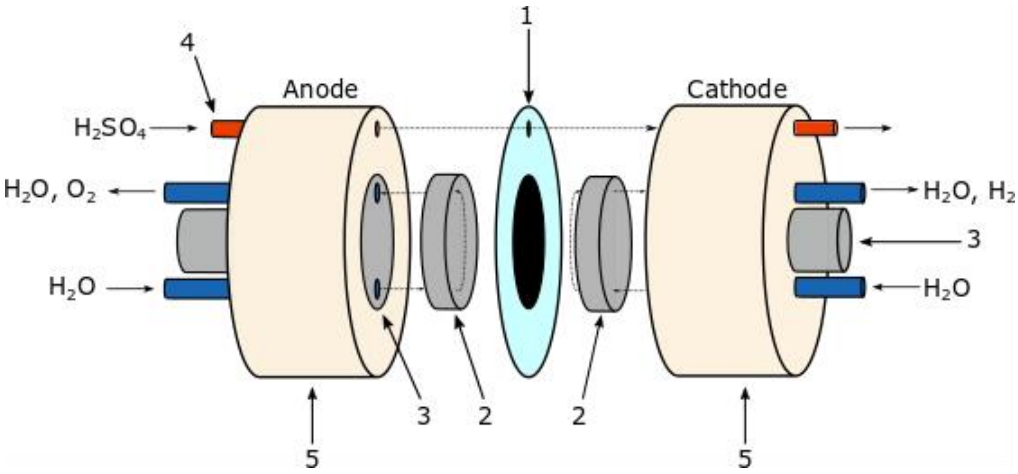

b)

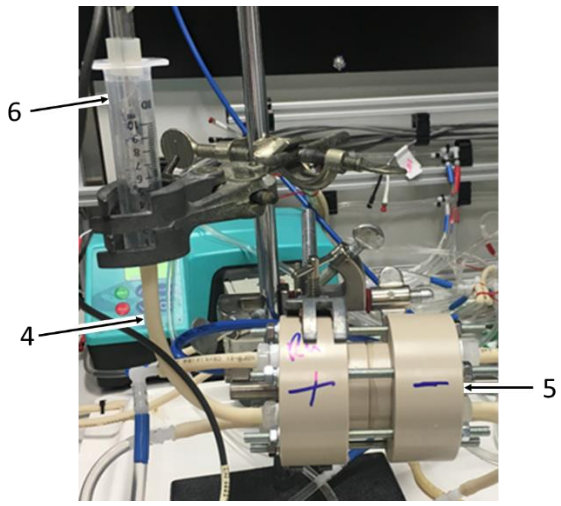

Figure S.I.1. Schematic of 3-electrode cell (a) and the cell setup (b). The cell design consists of CCM with a Nafion peripheral area acting as a gasket (1), gold-coated titanium gas diffusion layers (2), gold-coated titanium pistons (3), Luggin capillary (4) in ionic contact with the Hg / $HgSO_4$ reference electrode in a reservoir of 0.5 M H_2SO_4 (6). The cell is contained within polyetheretherketone (PEEK) cell halves (5) and compressed with threaded rods.

The PEMWE cell design in Figure S.I.1 had a 5 cm^2 circular active area, consisting of a CCM of design previously mentioned (1), a sintered titanium gas diffusion layer (GDL, Merelex Corporation TI-M-01-FM.2MMT, thickness 2 mm, average pore size 100 µm), a diamond titanium mesh (Goodfellow – TI008720) (2), and pneumatically actuated titanium pistons (3). Both (2) and (3) were coated with 1 µm gold (TEER coatings). In order to facilitate electrode potential measurements, ionic contact to the Nafion membrane in the CCM was made through a hole bored through the cell halves (4), the membrane around the sealing edge was pierced at the hole and filled with 0.5 M H_2SO_4. One end of the hole in the completed cell was connected to a reservoir containing a Hg / $HgSO_4$ reference electrode, and the other was closed off after H_2SO_4 had drained through it. Upon operation, the pistons were pneumatically driven with 150 N cm^{-2} pressure to bring the GDL and CCM into intimate contact. Electrochemical impedance measurements of the three-electrode cell were performed at a series of current densities up to 1 A cm^{-2}, which demonstrated that there was negligible iR drop caused by the positioning of the Luggin capillary outside of the CCM active area.

S.I.2 EIS data on cell series resistances

The 3-electrode PEMWE setup necessitated a test of the Luggin capillary for iR drop. Three separate values of R_s are calculable: R_s between the anode and reference electrode (R_s / A), between the cathode and reference electrode (R_s / C) and the anode and cathode (R_s / Cell). Several galvanostatic impedance measurements (GEIS) were taken between 0.01 A cm^{-2} and 1 A cm^{-2}, with a representative Nyquist plot at 1 A cm^{-2} given in Figure S.I.2, and the corresponding R_s values given in Figure S.I.3. From the Nyquist plots, the R_s is measurable as the lower Z_{real} (real resistance) value at which the curve crosses the real axis. In the case of the anode impedance measurement at high current density, the R_s value was not directly measurable, so R_s values were obtained by the fitting of the curves against a Randles equivalent circuit of a resistor followed by a resistor and capacitor in parallel (R_s + (R_{ct} / C_{dl})). GEIS tests were performed with cell conditions as stated in the experimental section. The AC current amplitude of each measurement was 10% of the DC current, with 10 points

per decade from 50 kHz to 100 mHz. Before each GEIS measurement, the cell was run at the corresponding current density for 5 minutes.

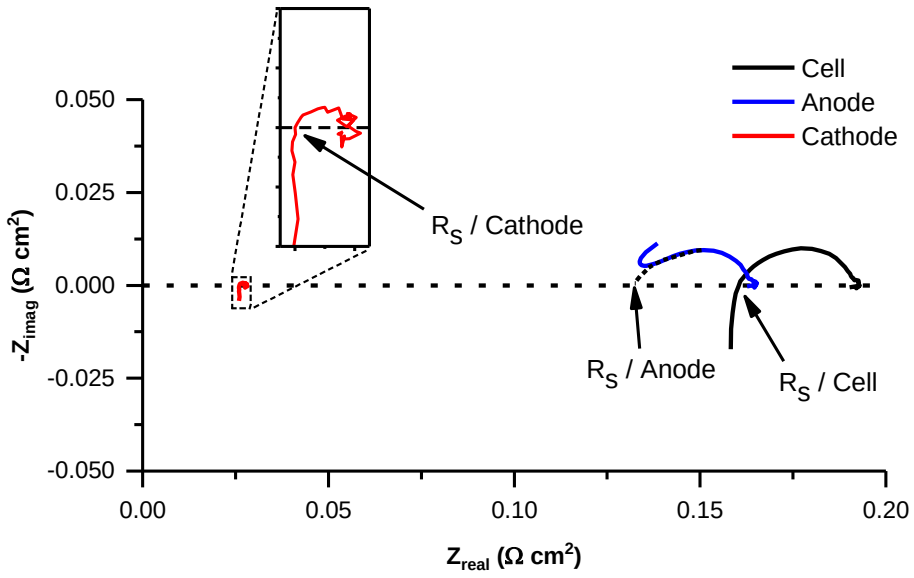

Figure S.I.2. Galvanostatic EIS at 1 Acm^{-2} of 3-electrode PEMWE cell

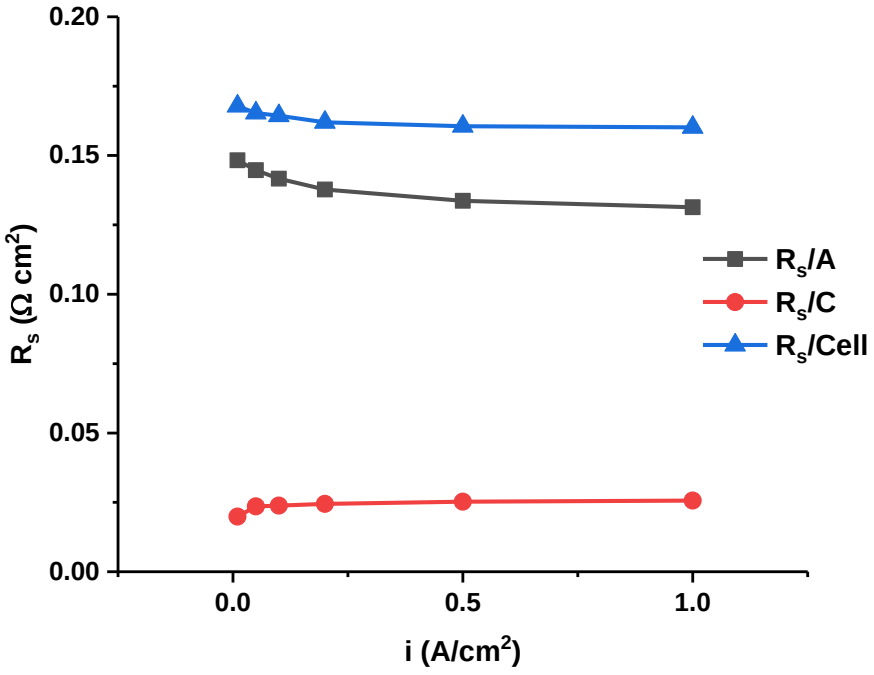

Figure S.I.3. R_s values for anode, cathode and cell from GEIS measurements

No significant change in R_s with current density was measured.

S.I.3 Limit of detection test, ICP-MS calibration curve and DPV profile

A limit of detection test was performed on both the DPV technique and ICP-MS using standard $PtCl_6^{2-}$ solutions with concentrations between 0.2 ng L^{-1} and 500 ng L^{-1} (Figure S.I.4). In this test DPV was shown to resolve Pt concentration at 2 ng L^{-1}, whereas ICP-MS was capable of resolving concentration at 50 ng L^{-1}.

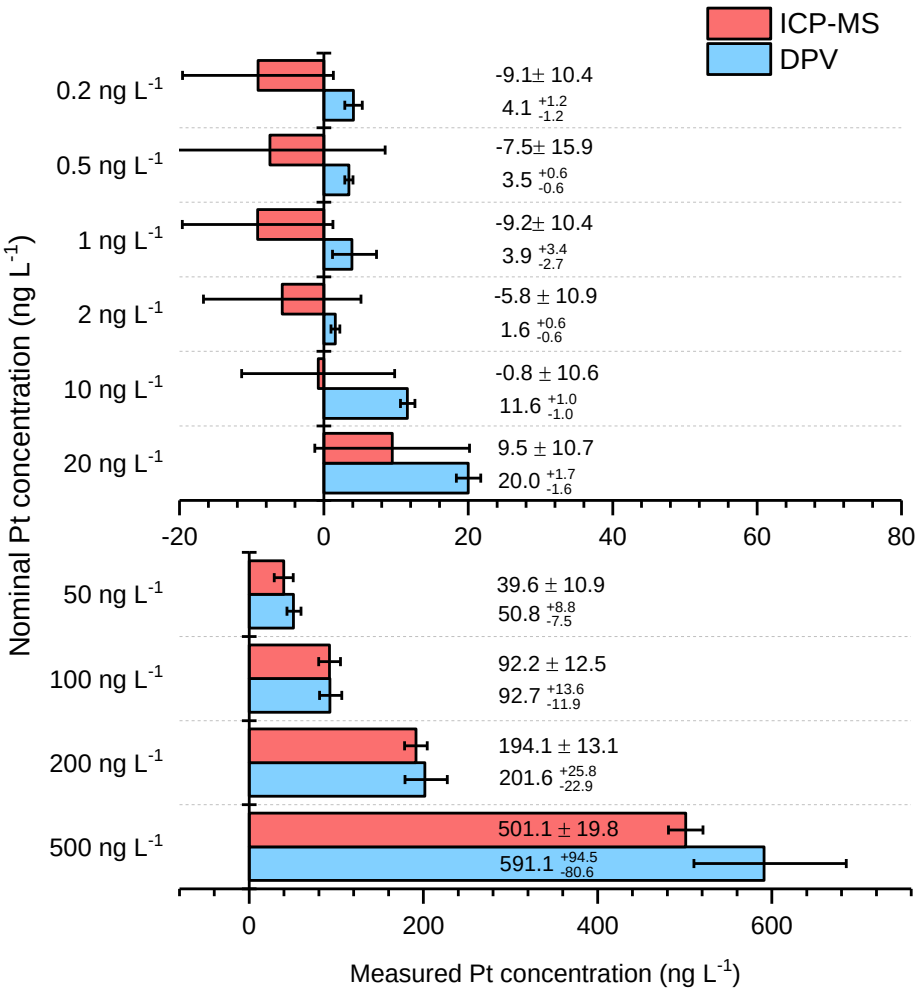

Figure S.I.4. Limit of detection tests of Pt standard solutions with DPV and ICP-MS

These standard solutions were measured in the same run as the PEMWE cathode water samples shown in Figure 1 in the main manuscript, and so were used as line of best fit against which the concentration of the PEMWE samples could be determined. The 0.2 – 20 ng L^{-1} Pt samples were used to produce the calibration curve in Figure S.I.5. Between each PEMWE cathode water sample measurement, the ICP-MS underwent several rinsing steps and measurement of a 1 ug L^{-1} standard solution, which was used to determine the variation in the signal strength for Pt. This variation was then offset in the water samples before measurement against the line of best fit.

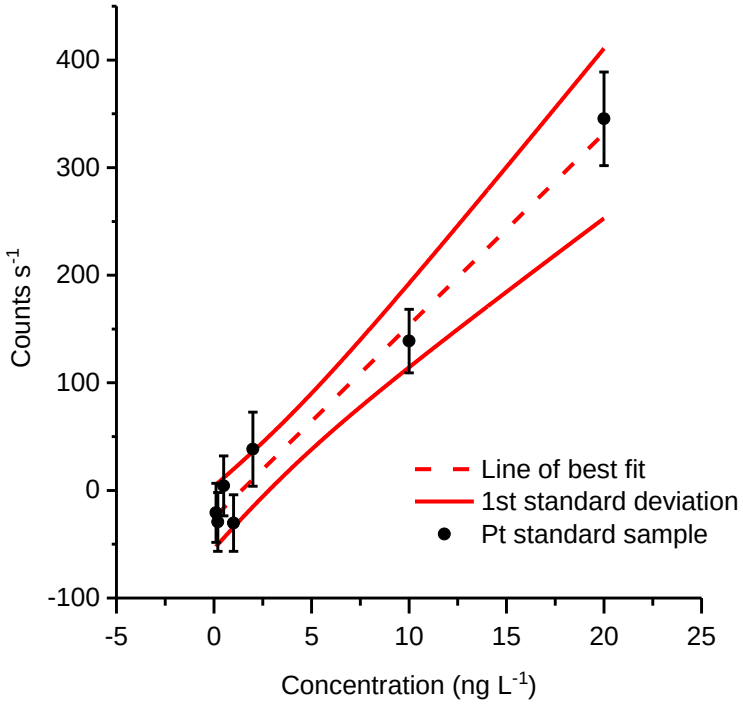

Figure S.I.5. ICP-MS calibration curve used for the fitting of ICP-MS data of Figure 1 in the main manuscript

In the DPV technique the rate of HER, which is a function of the Pt concentration, manifests as a current peak at approximately -0.88 V Ag / AgCl (Figure S.I.6). The maximum value of this peak is then subtracted from an approximation of the baseline for each DPV profile. At each concentration two DPV measurements are made. With the peak current values from the standard additions, a line of best fit of current against the increase in Pt concentration of the solution is calculated (Figure

S.I.7). The dilution of the sample by the supporting electrolyte is then factored in, and so the concentration of the initial sample is obtained.

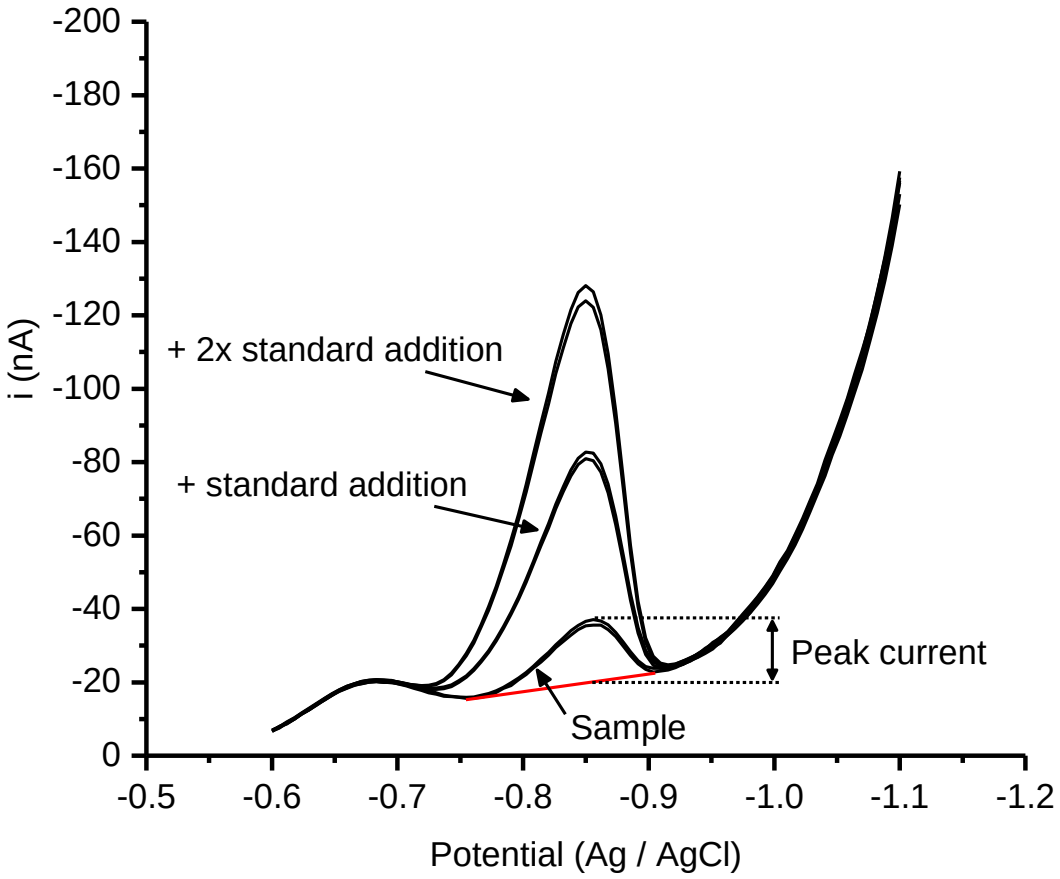

Figure S.I.6. DPV profiles of 2 ng L^{-1} Pt standard solution with the DPV profiles of the standard additions. The peak current is measured from a linear approximation of the baseline current (in red). The baseline is approximated separately for each DPV profile.

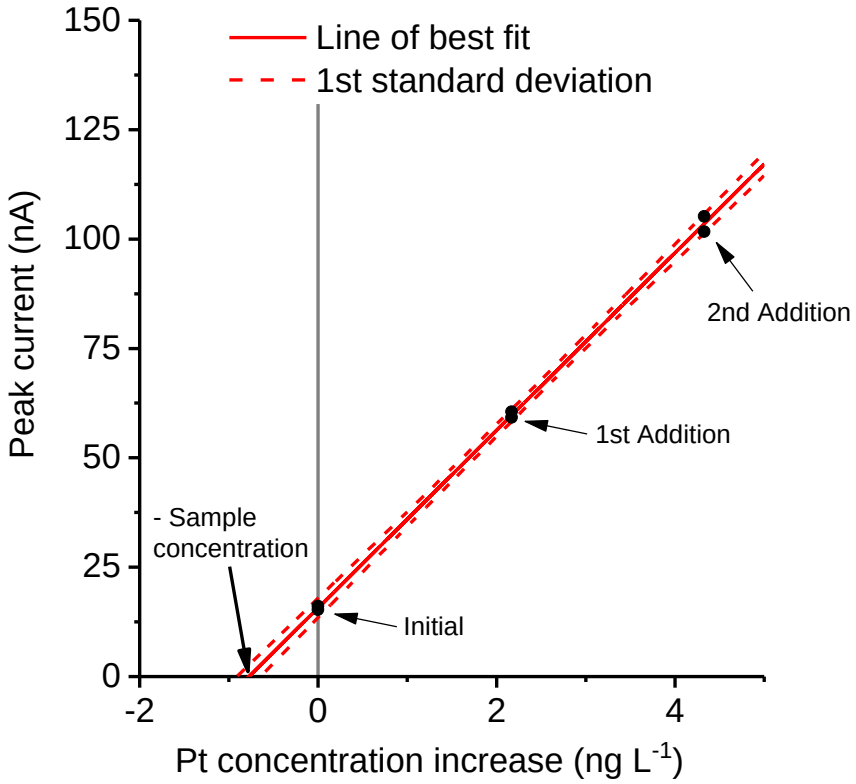

Figure S.I.7. Line of best fit of peak current values against the increase in Pt concentration of the sample. The concentration of the initial sample is the negative of the concentration value at 0 nA.

S.I.4 Repeat OCV profiles

The OCV dissolution test was performed three times on the same CCM in the same cell.

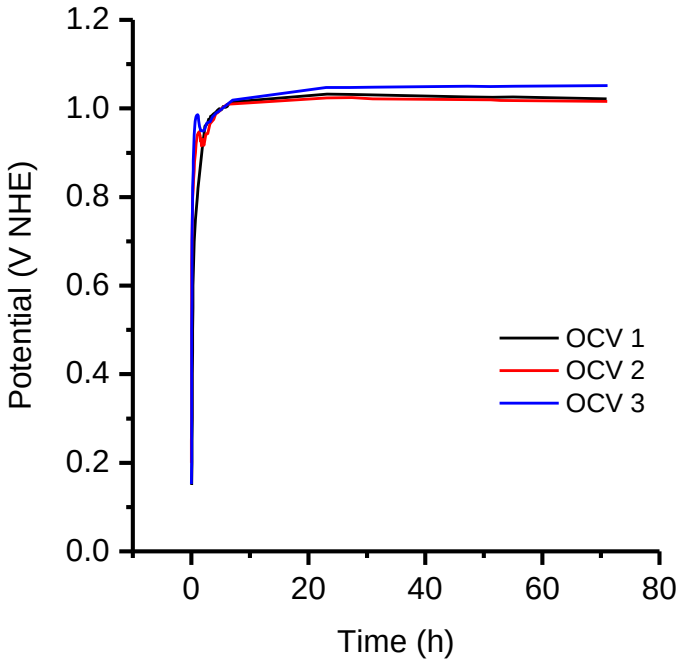

Figure S.I.8. Cathode potential of OCV tests during the OCV period

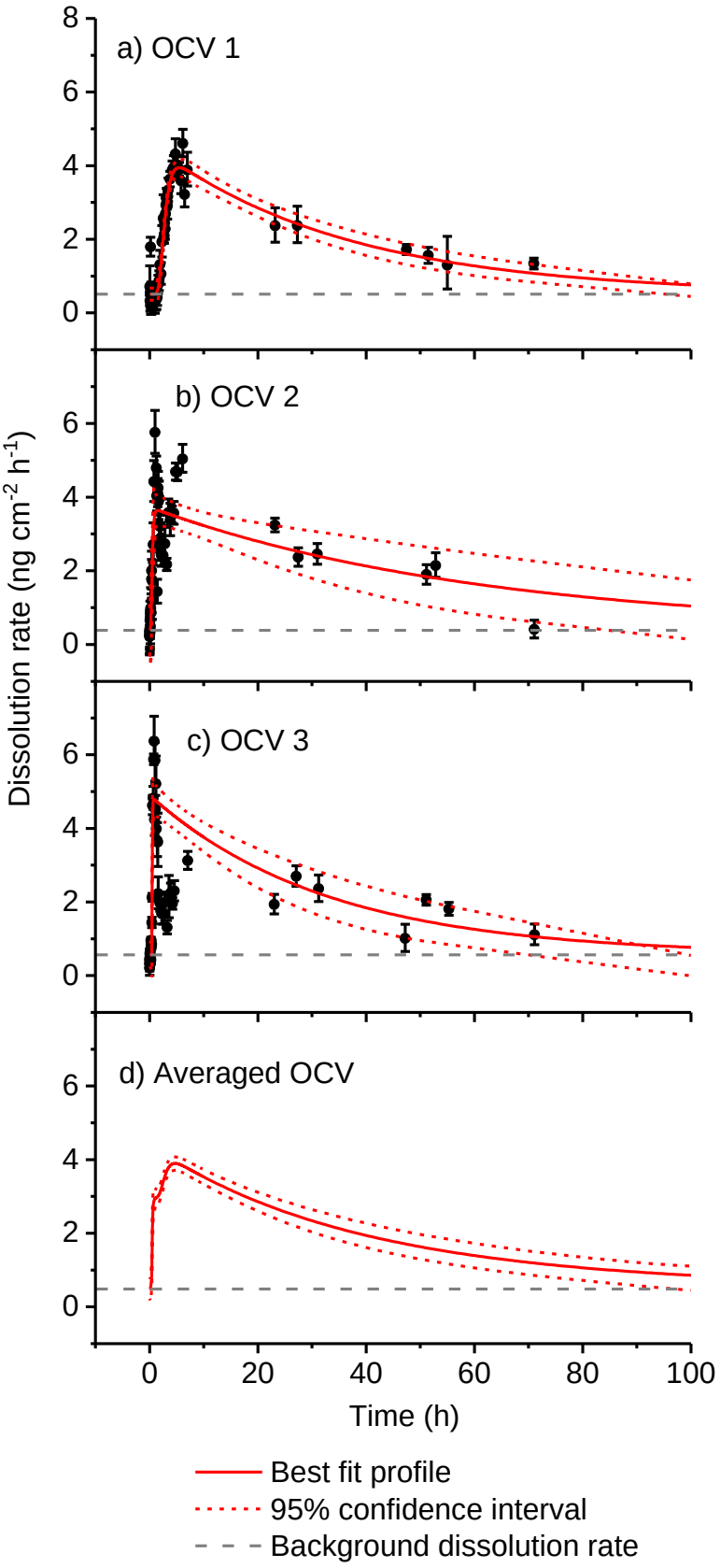

Figure S.I.9. Platinum dissolution rate from the PEMWE cathode over the full duration of the three OCV tests (a,b,c). Shown in (d) is the best fit of the individual best fit profiles.

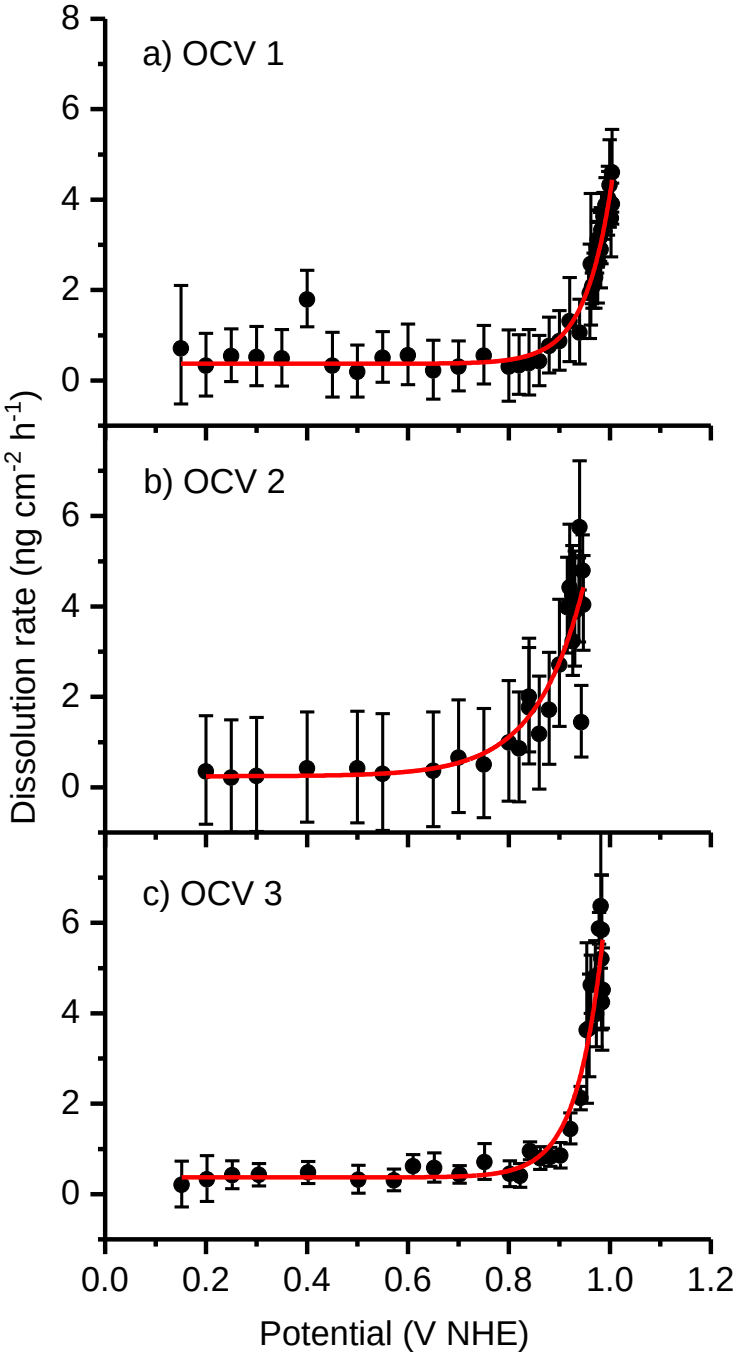

Figure S.I.10. Pt dissolution as a function of cathode potential of the three OCV tests.

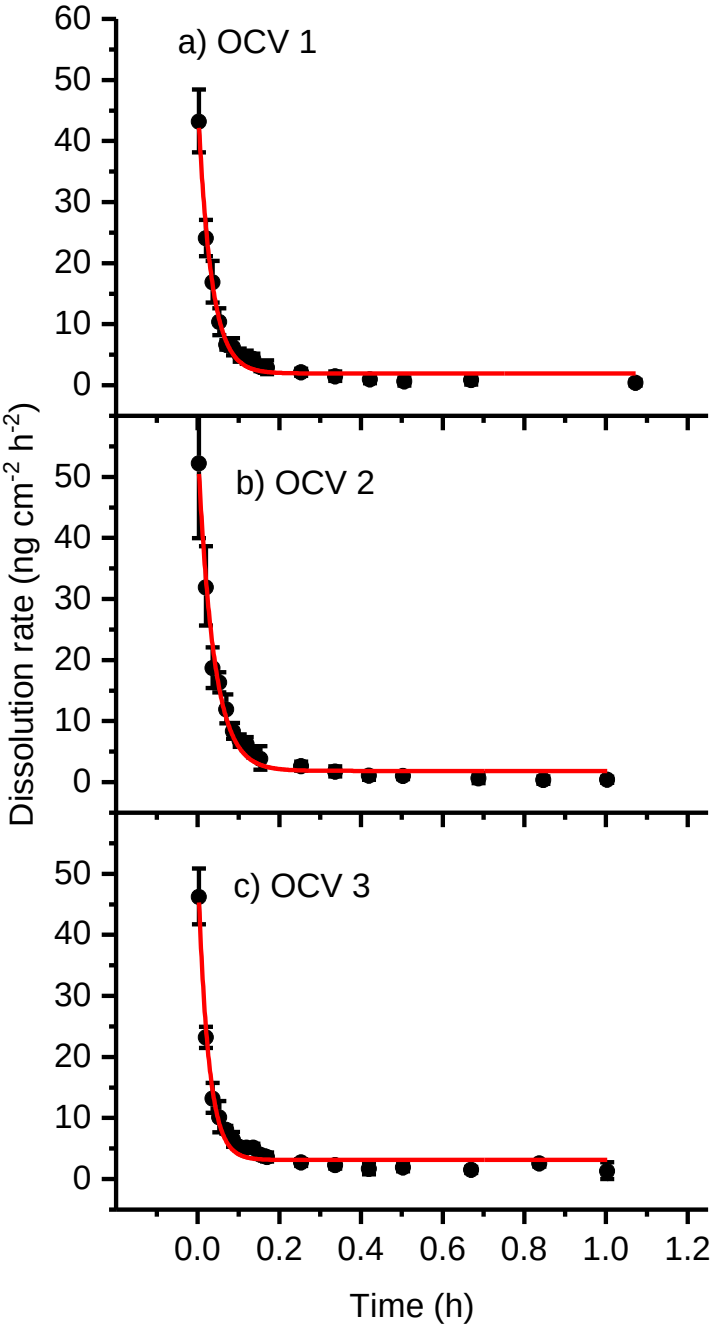

Figure S.I.11. The Pt dissolution rate of the three OCV tests from onset of operation at 1 A cm^{-2} immediately after the OCV period.

S.I.5. OCV dissolution forecasting

The Pt dissolution data during OCV were fitted against a pulse profile with equation (S.I.1).

(S.I.1) $$y = y_0 + A\left(1 - e^{\frac{-x}{t_1}}\right)^P e^{\frac{-x}{t_2}}$$

The profiles were fitted using the Levenburg-Marquadt algorithm to reach a chi-squared tolerance of 1×10^{-15}. The obtained values for each OCV plot are given in Table S.I.1. The fitted data is shown in Figure S.I.9.

Table S.I.1. Fitted values for Pt dissolution during OCV against a pulse profile. Results of this fitting are shown in Figure S.I.9.

	OCV 1			**OCV 2**			**OCV 3**		
	Value	Error	Dependency	Value	Error	Dependency	Value	Error	Dependency
y_0	0.5902	0.0827	0.7081	0.3874	0.3584	0.8727	0.5624	0.1543	0.5505
A	4.110	1.162	0.9934	3.457	359575	1	4.3821	15413	1
t_1	0.8038	0.2761	0.9972	0.1828	0.1285	0.9996	0.05609	0.05280	0.9994
P	25.00	368.1	0.9999	7.590×10^6	1.5×10^{12}	1	1.184×10^6	2.433×10^{12}	1
t_2	35.82	4.778	0.6131	61.45	24.57	0.4996	32.77	6.858	0.2864
R^2	0.952			0.722			0.913		

Pt dissolution values at the onset of operation after OCV were fitted against an exponential decay profile with equation (S.I.2). The profiles were fitted using the Levenburg-Marquadt algorithm to reach a chi-squared tolerance of 1×10^{-15}. The obtained values for each plot are given in Table S.I.2. The fitted data is shown in Figure S.I.11.

(S.I.2) $$y = y_0 + A\, e^{\frac{-x}{t_1}}$$

Table S.I.2. Fitted values for Pt dissolution during operation after the OCV period. Results of this fitting are shown in Figure S.I.11.

	OCV 1			**OCV 2**			**OCV 3**		
	Value	Error	Dependency	Value	Error	Dependency	Value	Error	Dependency
y_0	1.9375	0.3986	0.4501	1.849	0.567	0.4864	3.128	0.4294	0.3465
A	44.34	1.39	0.4004	52.76	1.809	0.4166	47.77	1.82	0.3873
t_1	0.03267	0.001950	0.5676	0.03868	1.678	0.5805	0.0254	0.0018	0.5107
R^2	0.988			0.987			0.984		

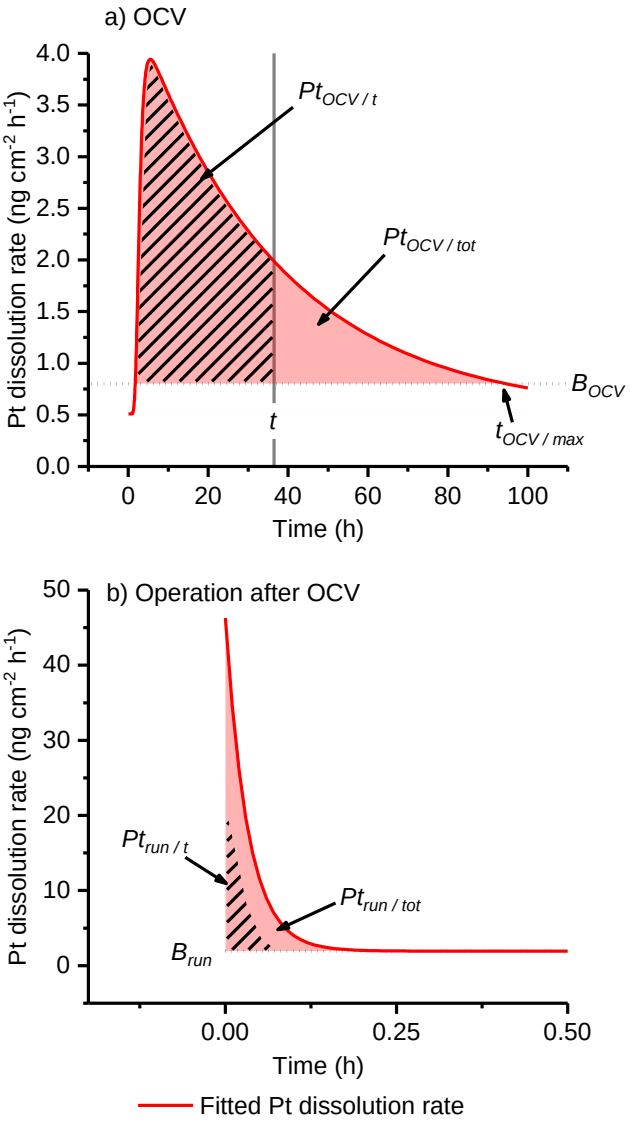

Figure S.I.12. Method used to forecast dissolution through OCV and operation after the OCV period

The average of the Pt dissolution rates for each OCV plot, as shown in Figure 5 in the main manuscript, were calculated in the following manner, with Figure S.I.12 included here as a guide: (1) The background Pt dissolution rates during OCV (B_{OCV}) and during operation (B_{run}) were established, and these values were assumed to be continuous throughout the duration of each test. (2) The fitted Pt dissolution rate data were subtracted from the respective background dissolution rates. The time at which it could no longer be stated with confidence that the fitted Pt dissolution rate was greater than the background dissolution rate was determined to be the time at which OCV dissolution ended

($t_{OCV\ /\ max}$). (3) The amount of total Pt dissolved during the OCV period in question ($Pt_{OCV\ /\ t}$) was integrated from the dissolution profile up to *t* hours. (4) The amount Pt dissolved during operation after OCV ($Pt_{run\ /\ tot}$) was obtained by integrating the operation dissolution profile. As it has been assumed that this dissolution rate is a product of OCV dissolution, for an OCV duration of *t*, the amount of Pt dissolved in this period ($Pt_{run\ /\ t}$) was calculated in the following manner:

(S.I.3) $$\theta = \frac{Pt_{OCV/t}}{Pt_{OCV/tot}}$$

(S.I.4) $$Pt_{run/t} = \theta\, Pt_{run/tot}$$

Furthermore, for the same reasons as mentioned above, it has been assumed that $Pt_{run\ /\ t}$ is not affected by the duration of operation. Therefore, for a complete OCV cycle of duration of *t* and operation period of t_{run}, the amount of Pt dissolved per cycle is calculated as follows:

(S.I.5) $$Pt_{cycle} = Pt_{OCV/t} + B_{OCV}t + \theta Pt_{run/tot} + B_{run}t_{run}$$

Table S.I.3. Pt dissolution amounts and estimations of the cathode electrode lifetimes at 3 mg cm^{-2} PtB

	OCV 1	**OCV 2**	**OCV 3**	**Average**
B_{OCV} (ng cm^{-2} h^{-1})	0.509 ± 0.167	0.388 ± 0.713	0.562 ± 0.315	0.486 ± 0.266
B_{run} (ng cm^{-2} h^{-1})	$1.937^{+0.855}_{-0.855}$	$1.849^{+1.216}_{-1.216}$	$3.128^{+0.915}_{-1.053}$	$2.305^{+0.582}_{-0.607}$
$t_{OCV\ /\ max}$ (h)	91.5	68.5	65	90
Pt_{cycle} (ng cm^{-2})	$123.8^{+27.2}_{-28.0}$	$136.2^{+66.4}_{-66.4}$	$120.1^{+39.4}_{-39.1}$	$152.44^{+61.9}_{-72.4}$
Pt dissolved during operation peak (ng cm^{-2})	$1.423^{+0.179}_{-0.181}$	$1.981^{+0.264}_{-0.666}$	$1.194^{+0.169}_{-0.1794}$	$1.533^{+0.323}_{-0.233}$
Max average OCV dissolution rate (ng cm^{-2} h^{-1})	$3.19^{+0.15}_{-0.26}$	$3.91^{+1.1}_{-0.66}$	$4.41^{+0.49}_{-0.46}$	$3.60^{+2.28}_{-1.84}$
Min average OCV dissolution rate (ng cm^{-2} h^{-1})	$0.52^{+0.51}_{-0.17}$	$0.50^{+0.76}_{-0.07}$	$0.63^{+0.34}_{-0.34}$	$0.59^{+0.74}_{-0.14}$
Most damaging cycle profile (h)	15.1	1.1	4.1	7.9
Minimum electrode lifetime (y)	$108^{+9.0}_{-6.0}$	$87.5^{+17.5}_{-19.1}$	$77.6^{+9.1}_{-7.7}$	$95.2^{+98.8}_{-36.9}$
Maximum electrode lifetime (y)	653^{+316}_{-383}	686^{+117}_{-413}	542^{+542}_{-190}	579^{+178}_{-321}